AIAA 80-1734R

Spin-Down and Active Nutation Controller for the Galileo Project

H.S. Lin*
Jet Propulsion Laboratory, California Institute of Technology, Pasadena, Calif.

A spin-down and active nutation controller (SDANC) stabilizes the Galileo spacecraft during spin-down from approximately 70 to 1 rpm. Angular motion of the spacecraft is sensed through a pair of accelerometers and a sun sensor which is needed only at low spin rates. Spin and nutation information is derived by a set of "loosely coupled" spin and transverse rate estimators. Spin rate is reduced by two spin-down thrusters. The transverse angular rate is compared with a variable threshold; exceeding the threshold activates axial thrusters that impart the appropriate transverse torque to reduce the nutation. The scheme was verified by extensive computer simulations and has been demonstrated over a wide range of initial conditions. The effect of energy dissipation was also included in the simulation by using the "energy sink method."

Introduction

THE object of this paper is to present a detailed design and analysis of an onboard nutation controller for a spacecraft having a prolate configuration. The scheme was originally designed for the Galileo spacecraft which was scheduled to be injected into a trajectory to Jupiter by a three-stage Inertial Upper Stage (IUS) booster. The IUS third stage was designed to be spin-stabilized at 50-70 rpm, with no active attitude control. After burnout, the third-stage/Galileo combination must be spun down to approximately 1 rpm for appendage deployment. The burned-out IUS and spacecraft is inertially prolate, spinning about its axis of least inertia (z axis), and is therefore dynamically unstable. The spin-down and active nutation controller (SDANC) contains the spacecraft nutation within a given threshold while reducing its spin rate. Spin-down is accomplished using a pair of spin thrusters which produce torque about the spin axis z (see Fig. 1). Nutation is controlled by timely firing of the axial thrusters (thrust vector along $-z$) to align the angular momentum with the spin axis, where the appropriate timing signals are derived from two digital integration accelerometers (ACC) and an acquisition sun sensor (AS). A similar nutation control scheme is discussed in Ref. 1 for the case where the spin rate is constant. The controller described in this paper differs significantly from that of Ref. 1 in implementation because of the spin rate variation (70-1 rpm).

System Description

A block diagram of a SDANC is shown in Fig. 2. The ACC READ and the AS READ subroutines process the outputs of the accelerometers and the acquisition sun sensor, respectively. The output of ACC READ is used in estimating the x and y components of the spacecraft angular rate, i.e., ω_x and ω_y, where x, y, z are body-fixed coordinates coinciding with the spacecraft principal axes. The transverse rate estimator (TRE) has the form of a Kalman filter. It estimates ω_x and ω_y, as well as any accelerometer misalignment. The outputs of TRE are used for two purposes. The estimated ω_y is input to the nutation control logic (NCL) and the estimated ω_x is fed to the zero cross-over detection logic (ZCD). The ZCD first checks the magnitude of the estimated transverse rate $\hat{\omega}_t$, which is defined as the mean square root of $\hat{\omega}_x$ and $\hat{\omega}_y$, where $\hat{\omega}_x$ and $\hat{\omega}_y$ are the estimated values of ω_x and ω_y. This is to assure the reliability of the estimated signals. The zero cross-over detection on $\hat{\omega}_x$ is performed only for the case when $\hat{\omega}_t$ exceeds a predetermined threshold. Protection is also built into the ZCD logic to prevent the possibility of multiple zero-crossings triggered by noise. The zero-crossing signal is used in estimating the spin rate prior to the availability of the sun acquisition signal. The AS output will not be available during the first few minutes of the spin-down because the trajectory of the flight puts the spacecraft in the Earth's shadow. If $\hat{\omega}_t$ does not pass the threshold test, the spin-down will not be performed until AS becomes available. The spin rate estimator (SRE) is designed to accept input from either AS READ or ZCD, but not both. In addition to estimating the spin rate, it also estimates the spin-down acceleration, α_z. The estimated spin rate is used to terminate the spin-down when the spin rate is reduced to 1 rpm. It is also used in computing the gains of the transverse rate estimator, which is performed in GAIN COMP block. The gains are chosen to be simple functions of spin rate and time in an effort to simplify the SDANC implementation. The nutation control logic receives inputs from the transverse rate estimator and compares the estimated transverse rate, $\hat{\omega}_y$, with a variable, multilevel deadband. It also commands the thruster logic (TL) to turn on

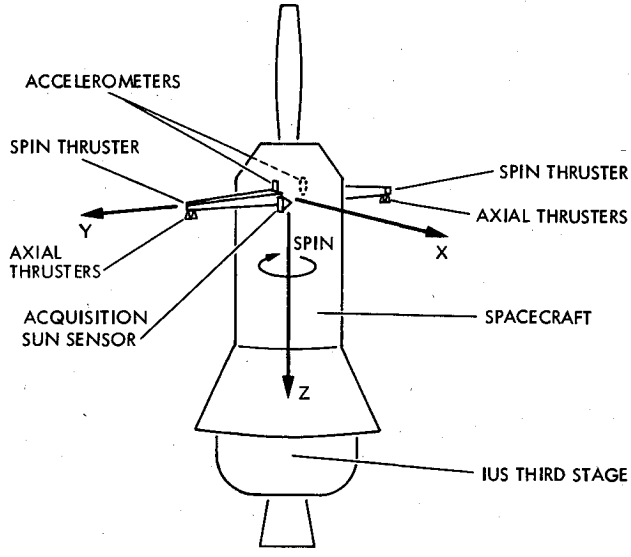

Fig. 1 Configuration of Galileo spacecraft.

Presented as Paper 80-1734 at the AIAA Guidance and Control Conference, Danvers, Mass., Aug. 11-13, 1980; submitted Oct. 27, 1980; revision received June 19, 1981.

*Member Technical Staff. Member AIAA.

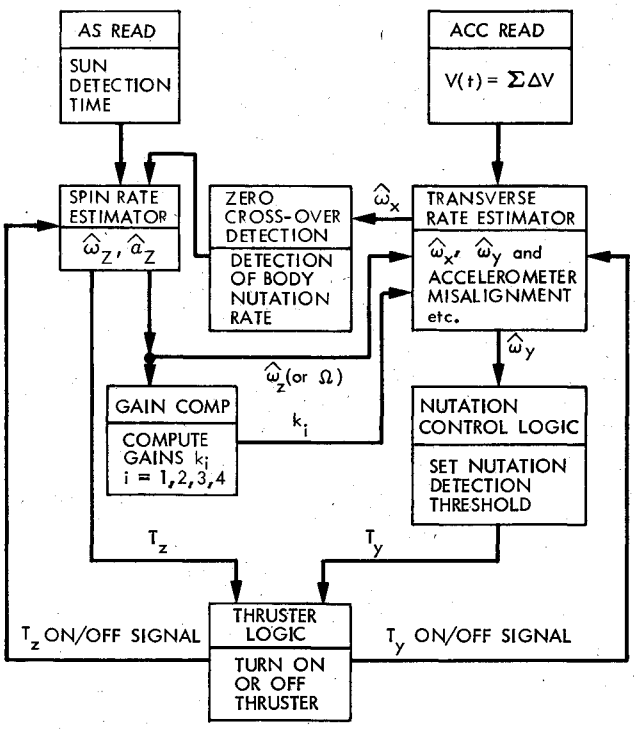

Fig. 2 Block diagram of spin-down and active nutation controller.

the axial thrusters whenever the deadband is exceeded. The nutation angle deadband is set and maintained at ±30 mrad prior to the time the AS is enabled. This will sustain some minor nutation motion and facilitate the spin rate estimation. After the AS is enabled, the deadband is gradually narrowed until the lower bound of ±2 mrad is reached. This logic for deadband narrowing is so designed that overcorrection of the transverse component of the angular momentum will not occur. The actual thruster turn-ons and turn-offs are controlled by the TL. A minimum thruster on-time of 25 ms is necessary for effective thruster performance.

In designing the SDANC, the following factors were taken into consideration:

1) Initial spin rate uncertainty—a variation of 20% from the nominal value is considered.

2) ACC misalignment with respect to the spacecraft (S/C) z axis—assumed to be less than 12 mrad.

3) S/C mass center location uncertainty—assumed to be less than 2 cm from the origin of spacecraft geometrical coordinates.

4) Thurster torque level uncertainty—a maximum thrust level uncertainty of 10% from its nominal value is considered.

In addition, the system should be able to function properly in the event of a single accelerometer failure. This implies that some constraint on the ACC location is required, which will be discussed later. Because of the limited memory capability of the onboard processor and the mission critical nature of the algorithm, it is essential that the design be simple and reliable. In the following sections, the detailed design and analysis of SDANC is presented.

Derivation of Sensor Output Equations

Two digital integration accelerometers with a resolution of 0.002 m/s/bit are used for detecting the angular motion of the spacecraft. The relation between the angular rate of the spacecraft and the ACC's output is derived in this section.

Let $\boldsymbol{i}$, $\boldsymbol{j}$, and $\boldsymbol{k}$ be unit vectors along the spacecraft body-fixed coordinates (x,y,z) defined by the principal axes, and $\boldsymbol{r}$ be the position vector of an accelerometer. The acceleration at point $\boldsymbol{r}$ can be expressed as

$$\boldsymbol{a}=a_x\boldsymbol{i}+a_y\boldsymbol{j}+a_z\boldsymbol{k}=(\dot{\boldsymbol{\omega}}\times\boldsymbol{r})+(\boldsymbol{\omega}\cdot\boldsymbol{r})\boldsymbol{\omega}-(\boldsymbol{\omega}\cdot\boldsymbol{\omega})\boldsymbol{r}+\boldsymbol{a}^0 \tag{1}$$

where ω is the angular rate, $\dot{\omega}$ is the rate of change of angular rate, and a^0 is the linear acceleration at the mass center. Eliminating $\dot{\omega}$ by using Euler's equations of motion for a single rigid body, we obtain

$$a_x=\left(\frac{I_z+I_y-I_x}{I_y}\omega_x\omega_z+\frac{M_y}{I_y}\right)r_z+\left(\frac{I_z+I_y-I_x}{I_z}\omega_x\omega_y-\frac{M_z}{I_z}\right)r_y$$
$$-(\omega_y^2+\omega_z^2)r_x+a_x^0 \tag{2}$$

$$a_y=\left(\frac{I_x+I_z-I_y}{I_z}\omega_x\omega_y+\frac{M_z}{I_z}\right)r_x+\left(\frac{I_x+I_z-I_y}{I_x}\omega_y\omega_z-\frac{M_x}{I_x}\right)r_z$$
$$-(\omega_z^2+\omega_x^2)r_y+a_y^0 \tag{3}$$

$$a_z=\left(\frac{I_x+I_y-I_z}{I_x}\omega_y\omega_z+\frac{M_x}{I_x}\right)r_y+\left(\frac{I_x+I_y-I_z}{I_y}\omega_z\omega_x-\frac{M_y}{I_y}\right)r_x$$
$$-(\omega_x^2+\omega_y^2)r_z+a_z^0 \tag{4}$$

In the above equations, I stands for the moment of inertia of the spacecraft, M is the applied torque, and the subscripts x, y, and z indicate the x, y, and z components of the referred symbol.

Let $\boldsymbol{c}$ be the unit vector which defines the orientation of the ACC and be represented by

$$\boldsymbol{c}\triangleq l\boldsymbol{i}+m\boldsymbol{j}+n\boldsymbol{k} \tag{5}$$

Then the output of the ACC will be

$$V=\sum\Delta V=\int_0^t\frac{\mathrm{d}V}{\mathrm{d}\tau}\mathrm{d}\tau=\int_0^t(la_x+ma_y+na_z)\mathrm{d}\tau \tag{6}$$

For the Galileo spacecraft, the two ACC's are located symmetrically with respect to z in the $y-z$ plane (i.e., $r_x=0$, $l=0$). The ACC's, both measuring the incremental velocity along the z axis, have a nominal misalignment angle of 12 mrad with respect to z (i.e., $n\cong1$, $m=0.012$). With these assumptions, Eq. (6) is reduced to

$$V=\int_0^t\left(-m\omega_z^2r_y+\frac{I_x+I_y-I_z}{I_x}r_y\omega_y\omega_z+a_z^0\right)\mathrm{d}\tau \tag{7}$$

In the above simplification, it was assumed that the transverse rates ω_x and ω_y are small. It was also assumed that $r_z\cong0$. Equation (7) can be obtained with fewer assumptions when both ACC's are available and the difference of two ACC's is used. In this case, the terms in Eq. (6) which contain the factors r_x or r_z are cancelled, and so is the axial acceleration a_z^0. Although this case is assumed in the following analysis, the SDANC is also designed so that it can tolerate a single accelerometer failure with some degradation.

Using Euler's equation about the x axis (for the case $M_x=0$, because the transverse torque is applied about the spacecraft body y axis only), Eq. (7) can be rewritten

$$V(t)=\int_0^t-(m\omega_z^2r_y)\mathrm{d}\tau+k_m[\omega_x(t)-\omega_x(0)]+\eta \tag{8}$$

where

$$k_m=\frac{I_x+I_y-I_z}{I_y-I_z}r_y \tag{9}$$

and $\omega_x(0)$ is the initial condition of the transverse rate ω_x. The term η is introduced as a catch-all term. Equation (8) is the foundation for nutation estimation.

In addition to the two ACC's, the acquisition sun sensor (AS) is also required at low spin rates for estimating the spin rate.

The AS is mounted on the spacecraft rotor. It has a 10-deg clock (about z) and approximately 180-deg cone (about x) field-of-view. Whenever the field-of-view rotates past the sun, a 10-deg width pulse is generated. The period between two consecutive sun acquisitions is not only a function of the spin rate, but also a function of the spacecraft nutation angle and the angle between the sun line and the spacecraft z axis (Ref. 2). Therefore the AS can only be used in estimating the spin rate when the nutation angle is small.

Estimation of the Angular Motion

The essence of the SDANC scheme is the estimation of spacecraft angular motion. For the sensor model given in the last section, at least six state variables are required for estimating the angular rate: three components of angular rate, ω_x, ω_y, and ω_z; the accelerometer (ACC) misalignment constant m; the accumulated ACC bias due to ACC misalignment β; and the thrust level of the spin-down thrusters T_z, which are on continuously but with a thrust level uncertainty of about 10%. Moreover, these state variables are described by a set of nonlinear differential equations. Therefore the estimation scheme, in general, is nonlinear with six state variables and is clearly unacceptable for onboard implementation. In this section, a different approach is considered.

Using the fact that the spin rate ω_z changes no faster than 1 deg/s^2, and that the nutation angle in general is small (<10 deg), the angular rate is estimated by a set of "loosely coupled" estimators—the transverse rate estimator and the

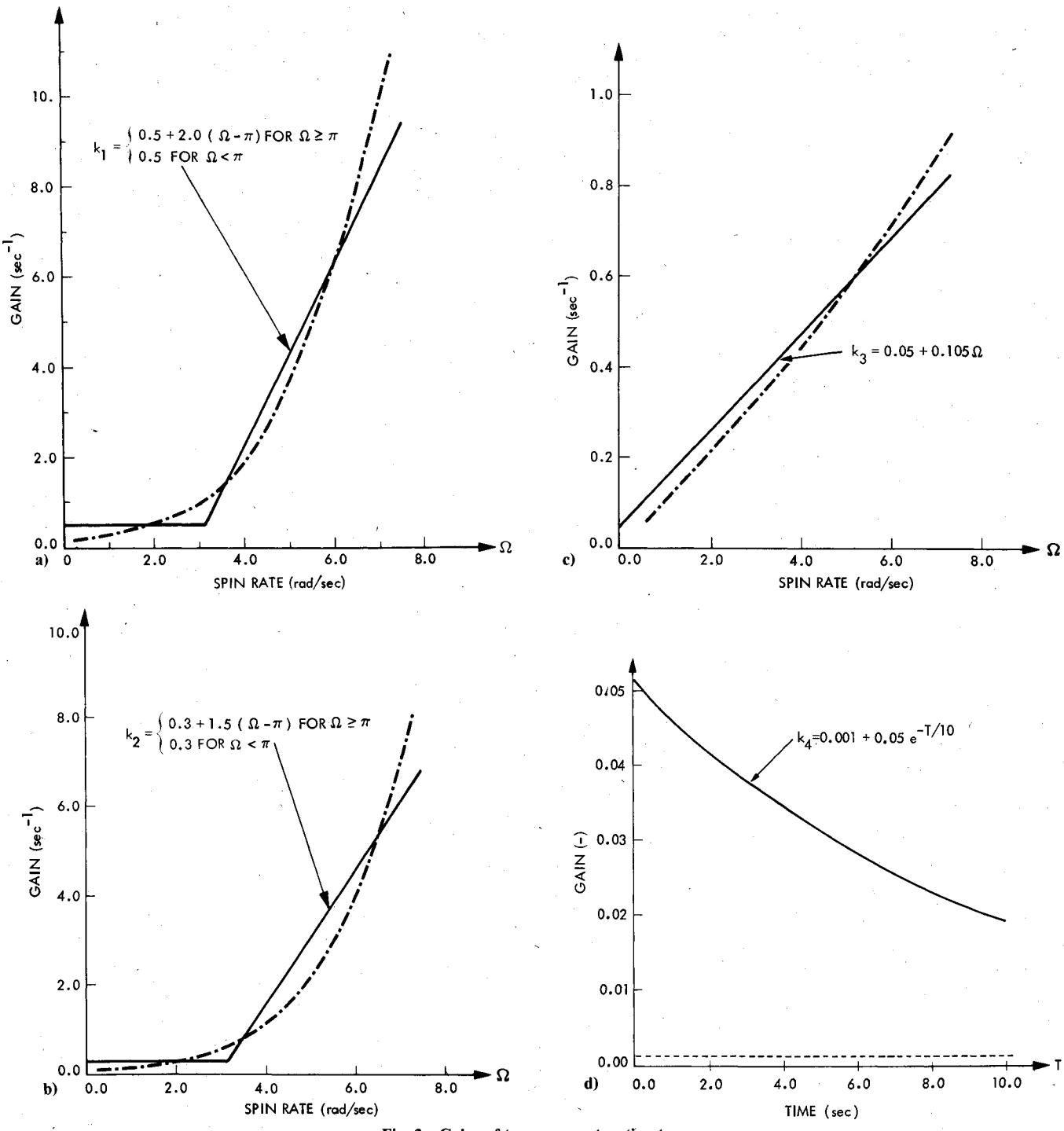

Fig. 3 Gains of transverse rate estimator.

spin rate estimator. The transverse rate estimator is designed by assuming the spin rate ω_z is "known." To emphasize the fact that the spin rate is "known," the symbol Ω is used for the estimated value of ω_z. The effect of the spin rate uncertainty is then considered. Finally, the spin rate estimator is designed to accept output either directly from the acquisition sun sensor or indirectly from the transverse rate estimator.

Formulation of the Transverse Rate Estimator

The relationship between the ACC's output and the spacecraft angular motion defined in Eq. (8) can be rewritten as

$$V(t)=k_m\omega_x(t)+\beta(t)+\eta \tag{10}$$

where

$$\dot{\beta}(t)\triangleq -m\omega_z^2 r_y \qquad \beta(0)=-k_m\omega_x(0) \tag{11}$$

Defining the state variable x as

$$x\triangleq\begin{bmatrix} x_1\\ x_2\\ x_3\\ x_4\end{bmatrix}\triangleq\begin{bmatrix} \omega_x\\ \omega_y\\ \beta/k_m\\ -mr_y/k_m\end{bmatrix} \tag{12}$$

we can rewrite Euler's equation for the transverse angular rates and the left-hand portion of Eqs. (11) in the form

$$\dot{x}=Fx+Gu+\mu \tag{13}$$

where

$$F=\begin{bmatrix} 0 & \dfrac{I_y-I_z}{I_x}\Omega & 0 & 0\\ \dfrac{I_z-I_x}{I_y}\Omega & 0 & 0 & 0\\ 0 & 0 & 0 & \Omega^2\\ 0 & 0 & 0 & 0\end{bmatrix} \tag{14}$$

$$G\triangleq[0\ 1\ 0\ 0]^T \qquad u\triangleq\alpha_y=M_y/I_y$$

$$\mu\triangleq[\mu_1\mu_2\mu_3\mu_4]^T$$

The variables μ_i are used to reflect the possible inaccuracy in the dynamical model. The state variable x_4 is introduced to deal with the possible error in the assumed ACC misalignment. Using the definition given in Eq. (12), the output observation $y(t)$ can be rewritten as

$$y=V/k_m=Hx+\mu_0 \tag{15}$$

where

$$H\triangleq[1\ 0\ 1\ 0] \qquad \mu_0\triangleq\eta(t)/k_m \tag{16}$$

Equations (12-16) form a standard estimation problem: based upon output measurements $y(t)$, in the interval $0\le t\le T$, estimate x. A least-squares criterion approach given in Ref. 3 is used in obtaining the result. The estimation is said to be the best if the following cost functional

$$J\triangleq\int_0^T[(y-H\hat{x})^2+\mu^TQ\mu]\,dt \tag{17}$$

is minimized. In the above equation, Q is the weighting matrix of the form

$$Q\triangleq\begin{bmatrix} q_1 & 0 & 0 & 0\\ 0 & q_2 & 0 & 0\\ 0 & 0 & q_3 & 0\\ 0 & 0 & 0 & q_4\end{bmatrix} \tag{18}$$

and μ satisfies the constraint given in Eq. (13). Using the invariant imbedding technique (Ref. 3), the optimal sequential estimator is obtained:

$$\dot{\hat{x}}=F\hat{x}+Gu+k(y-H\hat{x}) \tag{19}$$

where

$$k\triangleq[k_1k_2k_3k_4]=PH^T \tag{20}$$

and P is defined by the matrix Riccati equation

$$\dot{P}=FP+PF^T-PH^THP+Q^{-1} \tag{21}$$

For a given spin rate Ω and a predetermined matrix weighting function $Q(\Omega)$, a steady-state solution for P exists; i.e., the steady-state $k(\Omega)$ exists. This gain was obtained by computer simulations. The components of the gain are plotted in dotted lines in Figs. 3. These components are further approximated by simple functions (plotted in solid lines) for easy onboard implementation. The exponential term in Fig. 3d was introduced to accelerate the estimation of accelerometer misalignment. k_4 will be reduced to a small value when the estimated misalignment angle approaches its true value.

The selection of the weighting matrix Q needs further elaboration. The q_i's were chosen so that each component of the dynamical modeling error vector μ in the integrand of Eq. (17) carries the same weight as the term of the observation error, $y-H\hat{x}$. The observation error is caused primarily by the quantization error of the ACC. The dynamical modeling errors are further detailed as follows. The terms μ_1 and μ_2 reflect the error in spin rate estimation, the deviation of the assumed spacecraft inertia properties from their actual values, the possible variation in thrust level, and the effect of energy dissipation. These terms increase monotonically with the magnitude of the transverse rate ω_t. The term μ_3 is caused by the error in the spin rate estimation. This term increases in proportion to the accelerometer misalignment, which is predicted to be 12 mrad. In addition, the error in estimating linear acceleration during axial thruster firing should also be considered in case only a single accelerometer output is used. The term μ_4, in general, should be very small. It was chosen to be 10^{-6}. The values of the q_i's at various spin rates were determined with the following assumptions: 1) a 3% error in the assumed spacecraft moments of inertia, 2) a 10-mrad/s error in estimating the spin rate, 3) a 12-mrad accelerometer misalignment angle, 4) a 5% variation in thrust level with a thruster duty cycle of 40%, and 5) the nominal operating points given in Table 1.

In the above discussion, the uncertainty in the parameter k_m, defined in Eq. (9), is not considered. An error in this parameter has the same effect as an error in the accelerometer's scale factor. This effect causes the estimated rate error to vary proportionally with these errors.

Effect of Spin Rate Uncertainty

In deriving the transverse rate estimator, it was assumed that the spin rate is known. In this paragraph, the effect of unknown spin rate is briefly discussed. To simplify the analysis, it is assumed that all system parameters, i.e., inertia properties, etc., are known, and the ACC's are aligned with

Table 1 Nominal operating points

Spin rate, rpm	70	60	50	40	30	20	10	5
Nutation angle, deg	3.5	3.0	2.5	2.0	1.5	1.0	0.5	0.25

the spacecraft z axis. With these assumptions, and neglecting the observation error, the estimated transverse rates can be written as

$$\dot{\hat{\omega}}_x = A\hat{\omega}_y\Omega + k_1(\omega_x - \hat{\omega}_x) \qquad \dot{\hat{\omega}}_y = B\hat{\omega}_x\Omega + \alpha_y + k_2(\omega_x - \hat{\omega}_x) \tag{22}$$

where

$$A \triangleq (I_y - I_z)/I_x > 0 \qquad B \triangleq (I_z - I_x)/I_y < 0 \tag{23}$$

Defining the estimation error as

$$\omega_{xe} \triangleq \hat{\omega}_x - \omega_x \qquad \omega_{ye} \triangleq \hat{\omega}_y - \omega_y \tag{24}$$

and using Euler's equation for the transverse angular rates ω_x and ω_y, we obtain

$$\dot{\omega}_{xe} = A\omega_{ye}\Omega + A\omega_y(\Omega - \omega_z) - k_1\omega_{xe}$$

$$\dot{\omega}_{ye} = B\omega_{xe}\Omega + B\omega_x(\Omega - \omega_z) - k_2\omega_{xe} \tag{25}$$

Assuming that the spin rate is constant, Eqs. (25) can be combined:

$$\ddot{\omega}_{xe} + k_1\dot{\omega}_{xe} - A\Omega(B\Omega - k_2)\omega_{xe} = A\dot{\omega}_y(\Omega - \omega_z) + AB\Omega(\Omega - \omega_z)\omega_x \tag{26}$$

At high spin rate and for a sufficiently large nutation angle, i.e., $\omega_x\omega_z \gg \alpha_y$, Eq. (26) can be rewritten as

$$\ddot{\omega}_{xe} + k_1\dot{\omega}_{xe} - A\Omega(B\Omega - k_2)\omega_{xe} = AB(\Omega^2 - \omega_z^2)\omega_x \tag{27}$$

where the right side of Eq. (27) is derived by using Euler's equation about the y axis. The solution of Eq. (27) takes the form

$$\omega_{xe} = \frac{AB(\Omega^2 - \omega_z^2)\omega_x}{\{[AB(\omega_z^2 - \Omega^2) + (A\Omega k_2)]^2 - k_1^2 AB\omega_z^2\}^{1/2}} \angle -\theta_f + e^{-(k_1/2)t}\{\omega_{xe}(0)\cos\omega_n t + (1/\omega_n)[\dot{\omega}_{xe}(0) + (k_1/2)\omega_{xe}(0)]\sin\omega_n t\} \tag{28}$$

where

$$\theta_f = \tan^{-1}\frac{k_1\sqrt{-AB\omega_z}}{[AB(\omega_z^2 - \Omega^2) + A\Omega k_2]}\omega_n = [A\Omega(k_2 - B\Omega) - k_1^2/4]^{1/2} \tag{29}$$

At the nominal initial spin rate of 50 rpm, the gains k_1 and k_2 are computed to be 4.69 and 3.40, respectively. Therefore the transient term will be negligible within 2 s, while the actual spin rate change is less than 2 deg/s, or approximately 0.35% of the initial spin rate. The steady-state estimation error ω_{xe} has the same frequency as the actual transverse rate ω_x. Therefore the estimated ω_x, $\hat{\omega}_x$, has the same frequency as ω_x even if the spin rate assumed in the transverse rate estimator was not accurate. For this reason, at a high spin rate, the estimated transverse rate, $\hat{\omega}_x$, is used in estimating the spin rate.

From Eqs. (28) and (29), it is found that for an actual spin rate, ω_z, of 60 rpm, and an estimated spin rate, Ω, of 50 rpm, the actual and estimated rates, ω_x and $\hat{\omega}_x$, are related by the following equation:

$$\hat{\omega}_x = \omega_x + \omega_{xe} = 1.069 \angle -7.5 \text{ deg } \omega_x \tag{30}$$

which indicates a 6.9% error in the nutation angle estimation and a phase shift of about -7.5 deg. This estimated rate is sufficiently accurate for the nutation control.

Spin Rate Estimator

Both the accelerometers (ACC's) and the acquisition sun sensor (AS) are needed in estimating the spin rate of the spacecraft. The ACC's provide the spin rate information when the spacecraft is not in a pure-spin state. It is used in the initial spin-down when the AS output is not available. The AS is needed only at low spin rates and can accurately measure the spin rate, provided the nutation angle is small. The dynamics of spin rate variation are given by Euler's equation (about the z axis) as

$$\dot{\omega}_z = [(I_x - I_y)/I_z]\omega_x\omega_y + M_z/I_z \tag{31}$$

The first term on the right side of Eq. (31) can be neglected in general. This is because of the fact that the spacecraft is almost symmetrical about the spin axis, i.e., $I_x \cong I_y$, and the nutation angle in general is small (<2 deg). In case the spin rate is estimated from the estimated transverse angular rate, $\hat{\omega}_x$, the integration of the $\omega_x\omega_y$ term over an entire observation period (i.e., the period between two consecutive zero-crossing times of the estimated rate, $\hat{\omega}_x$) is small, even if the term $\omega_x\omega_y$ itself is not small. For these reasons, Eq. (31) can be reduced to

$$\dot{\omega}_z = M_z/I_z + \mu_5 \triangleq \alpha_z + \mu_5 \tag{32}$$

To deal with the uncertainty in the knowledge of the despun torque, α_z is also included in the estimation

$$\dot{\alpha}_z = \mu_6 \tag{33}$$

Equations (32) and (33) can be written in the discrete form as

$$\omega_z(t_{k+1}) = \omega_z(t_k) + \alpha_z(t_k)\Delta t_k + \mu_5(t_k)$$

$$\alpha(t_{k+1}) = \alpha_z(t_k) + \mu_6(t_k) \tag{34}$$

Assuming that the times t_k for $k = 0,1,2,\ldots$ correspond to the times that the AS passes the sun or the times that a zero transverse rate, $\hat{\omega}_x$, is detected, the following observation equation is obtained.

$$2p\pi = \omega_z(t_k)\Delta t_k + \tfrac{1}{2}\alpha_z(t_k)(\Delta t_k)^2 + \mu(t_{k+1}) \tag{35}$$

where

$$p = 1 \quad \text{when AS is used} \qquad = 0.5/\sqrt{-AB} \quad \text{otherwise} \tag{36}$$

$$\Delta t_k = t_{k+1} - t_k$$

and $\mu(t_{k+1})$ is the observation error. From Eqs. (34-36), an estimator of the following form is chosen.

$$\hat{\omega}_z(t_{k+1}) = \hat{\omega}_z(t_k) + \hat{\alpha}_z(t_k)\Delta t_k + k_5(t_{k+1})e(t_{k+1})$$

$$\hat{\alpha}_z(t_{k+1}) = \hat{\alpha}_z(t_k) + k_6(t_{k+1})e(t_{k+1}) \tag{37}$$

where

$$e(t_{k+1}) = 2p\pi - \hat{\omega}_z(t_k)\Delta t_k - \tfrac{1}{2}\hat{\alpha}_z(t_k)(\Delta t_k)^2 \tag{38}$$

The gains $k_5(t_{k+1})$ and $k_6(t_{k+1})$ are chosen to be

$$k_5(t_{k+1}) = k_s|\hat{\omega}_z(t_k)|/D(t_k)$$

$$k_6(t_{k+1}) = k_s|\hat{\alpha}_z(t_k)|/D(t_k) \tag{39}$$

where k_s is a proportional constant and is set to be 0.3, based on computer simulation. $D(t_k)$ is defined as

$$D(t_k) \triangleq |\hat{\omega}_z(t_k)\Delta t_k| + |\tfrac{1}{2}\hat{\alpha}_z(t_k)(\Delta t_k)^2| \tag{40}$$

These gains are chosen so that the error at every sampling time is reduced according to the weight of each influencing factor, $\hat{\omega}_z(t_k)$ and $\hat{\alpha}_z(t_k)$. The convergence of the scheme was verified by computer simulation. In the actual implementation, a preset boundary for $\hat{\alpha}_k$ is also included to prevent the estimated control acceleration from reaching an unreasonable value.

Verification

The performance of the SDANC was evaluated by extensive computer simulations. The dynamical model of the spacecraft was assumed to be rigid. The effect of energy dissipation was introduced by using the "energy sink method," which will be further elaborated on in a subsequent section. Parameters pertaining to the Galileo spacecraft were used in the simulation. Computer simulations for many sets of different initial conditions were performed. The results are summarized in the following sections.

Range of Convergence

In designing the SDANC estimators, it was assumed that the spacecraft nutation angle is small. However, due to the fact that the spacecraft is almost symmetrical with respect to the z axis ($I_x \cong I_y$), the estimators, in reality, converge for a nutation angle as large as 30 deg. The results are demonstrated in Figs. 4 and 5. Figure 4 plots the actual and estimated transverse rates, ω_x and $\hat{\omega}_x$. The large estimation error in the first 5 s of the simulation is caused by the more than 10% over-estimate in spin rate. This figure also indicates that the nutation angle is reduced at a satisfactory rate. Figure 5 shows the actual and estimated spin rates. The initial spin rate is 40 rpm, and the estimated spin rate is 50 rpm. The estimated rate decreases linearly for the first 10 s because of the fact that only the thruster on-off signal is available at that time. The output of the transverse rate estimator, which is used in estimating the spin rate, is not available until 10 s later, when the transient of the transverse rate estimator is sufficiently reduced. The result of the simulation indicates that a better than 1% spin rate estimation accuracy can be obtained. From these results it is concluded that the SDANC will function properly for a nutation angle as large as 30 deg, provided that the nutation buildup due to energy dissipation is negligible.

Performance at Low Spin Rates

One of the major requirements for SDANC design is to reduce the spin rate to 1 rpm and maintain a nutation angle as small as possible to facilitate boom deployment. The performance of SDANC at low spin rates is demonstrated in

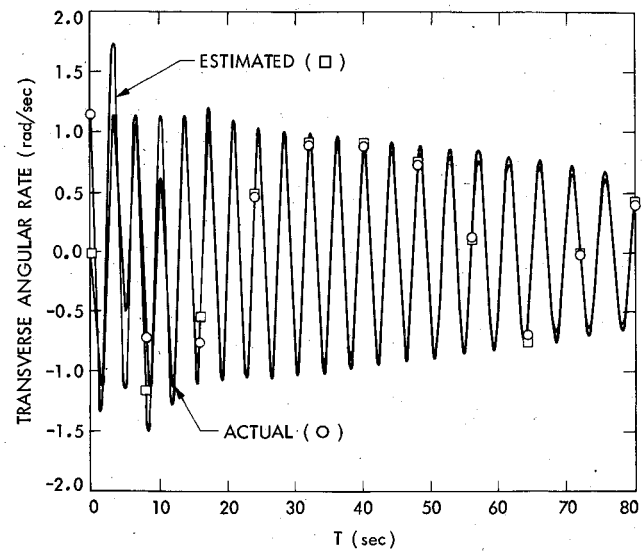

Fig. 4 Actual and estimated transverse rates at high spin rates.

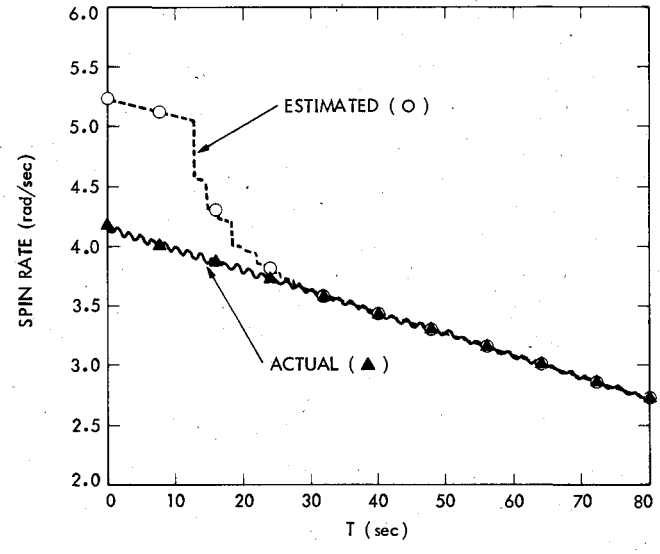

Fig. 5 Actual and estimated spin rates at high spin rates.

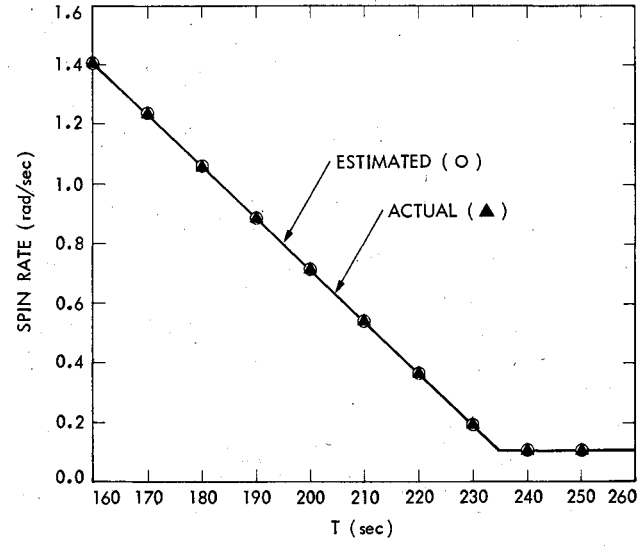

Fig. 6 Actual and estimated spin rates at low spin rates.

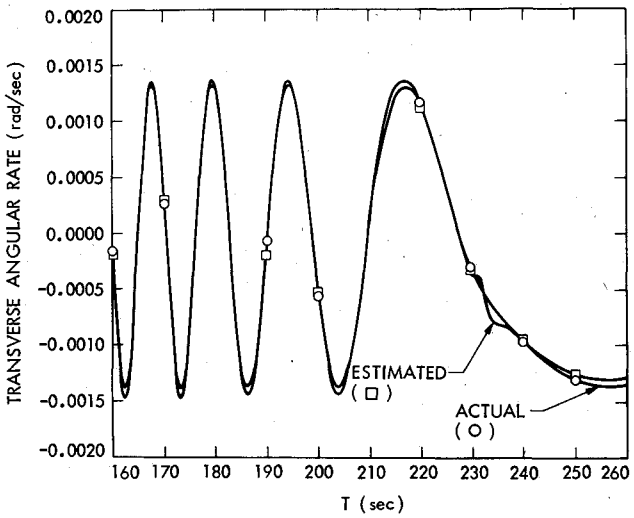

Fig. 7 Actual and estimated transverse rates at low spin rates.

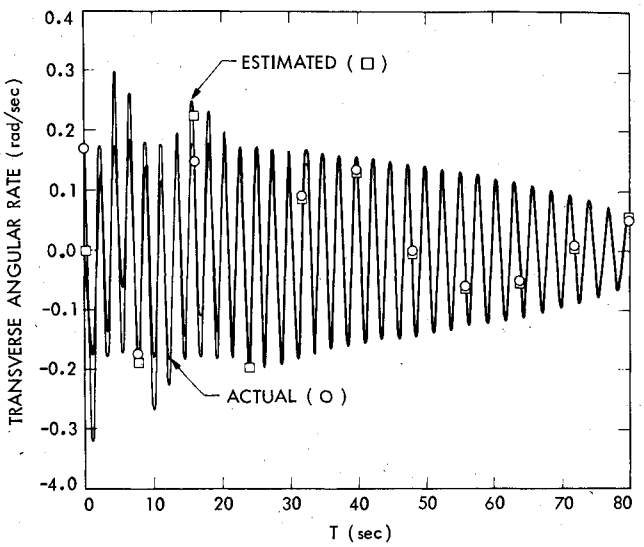

Fig. 8 Actual and estimated transverse rates for a stable case of energy dissipation

Figs. 6 and 7. In Fig. 6, the actual and estimated spin rates are plotted. The result indicates that the spin-down is terminated at 1 rpm with an error of less than 2%, which meets the design requirement. Figure 7 shows the actual and estimated transverse rates, ω_x and $\hat{\omega}_x$. The transverse rate ω_x is reduced to less than 2 mrad/s, which corresponds to a nutation angle of 2 deg at a spin rate of 1 rpm. The estimated rate closely follows the actual rate until the latter is reduced to 2 mrad/s. The degradation in estimator performance at low spin rates is caused primarily by insufficient accelerometer resolution (0.002 m/s/bit). This sets the lower bound for the threshold of the nutation control logic. The thrusters will not be fired whenever the transverse rate ω_y is reduced below 2 mrad/s.

Effect of Energy Dissipation

In the above simulation, the effect of energy dissipation was not included. Since SDANC is designed to prevent nutation buildup as a result of energy dissipation, this effect must be studied. The energy dissipation is caused primarily by fuel slosh. The Galileo spacecraft has four fuel tanks. The fuel slosh effect of these tanks has not been well understood. In order that the energy dissipation effect may be simulated, the dynamical model defined by the following equations is constructed:

$$\dot{\omega}_x = \frac{I_y - I_z}{I_x}\omega_y\omega_z + \frac{M_x}{I_x} + \dot{T}\frac{\omega_x}{(I_x - I_x^2/I_z)\omega_x^2 + (I_y - I_y^2/I_z)\omega_y^2} \tag{41}$$

$$\dot{\omega}_y = \frac{I_z - I_x}{I_y}\omega_z\omega_x + \frac{M_y}{I_y} + \dot{T}\frac{\omega_y}{(I_x - I_x^2/I_z)\omega_x^2 + (I_y - I_y^2/I_z)\omega_y^2} \tag{42}$$

$$\dot{\omega}_z = \frac{I_x - I_y}{I_z}\omega_x\omega_y + \frac{M_z}{I_z} - \dot{T}\frac{I_x^2\omega_x^2 + I_y^2\omega_y^2}{\omega_z I_z[(I_x I_z - I_x^2)\omega_x^2 + (I_y I_z - I_y^2)\omega_y^2]} \tag{43}$$

In the above equations, $\dot{T}$ is the rate of energy dissipation in watts. The model has the following properties: 1) Clearly, the above equations reduce to Euler's equations when there is no dissipation; i.e., $\dot{T}=0$. 2) It can be easily proved that for the torque-free case, the angular momentum of the system is conserved. 3) The rate of energy dissipation for the system equals $\dot{T}$.

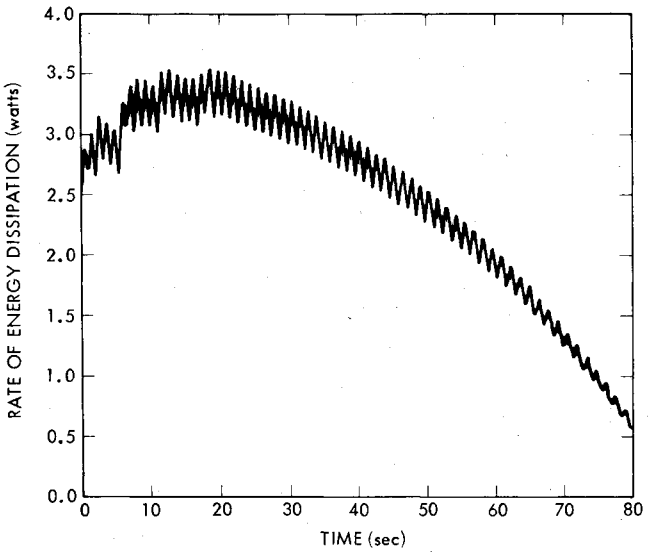

Fig. 9 Rate of energy dissipation for the stable case.

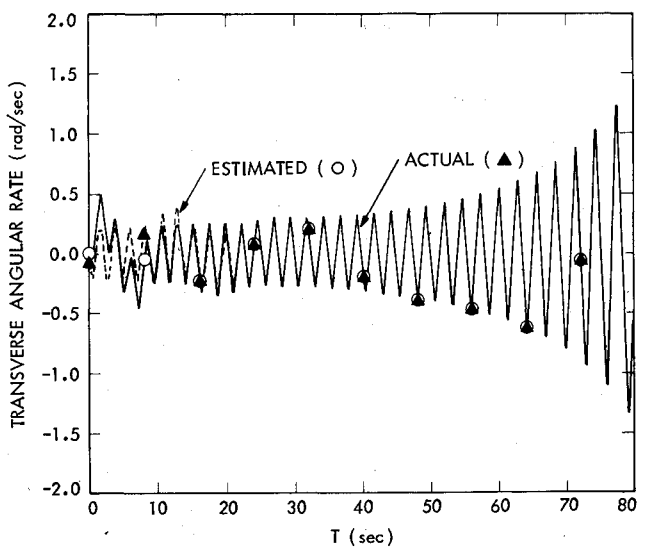

Fig. 10 Actual and estimated transverse rates for an unstable case of energy dissipation.

The above properties may not be sufficient to justify the correctness of the model. However, it does produce the nutation buildup effect which is needed in the simulation. The accuracy of the model will be verified when the Galileo fuel slosh effect is better understood.

The rate of energy dissipation is assumed, for lack of better information, to be of the form

$$\dot{T} = -\lambda\theta_n^2 \tag{44}$$

where θ_n is the nutation angle, and λ is a positive constant (for a given spin rate). For various levels of energy dissipation, the capability of SDANC was evaluated by simulation. The initial conditions assumed in the simulation are that the initial spin rate is 60 rpm and the initial nutation angle is 3 deg.

The results of the simulations are summarized in Figs. 8-10. Figures 8 and 9 show the simulation results of a stable case, which corresponds to an initial energy dissipation rate of about 2.5 W at a nutation angle of 3 deg. The increase in the nutation angle (Fig. 8) in the first 10 s is due to the initial estimation error. Figure 9 shows the power dissipation in watts. The power dissipation approaches zero after the nutation angle has been sufficiently reduced. For an energy dissipation rate larger than 2.5 W, the system becomes unstable. This is shown in Fig. 10, which corresponds to an initial energy dissipation of 2.8 W. One thing may be worth noticing in the figure—while the system becomes unstable, the estimated rate does not deviate much from the actual rate. In other words, the failure in the control scheme is due entirely to insufficient control torque.

Conclusion

The performance of the spin-down and active nutation controller was proved to be satisfactory, as shown in the simulations. It was shown by simulation that the "loosely coupled" transverse rate and spin rate estimators converge for an estimated initial spin rate error as large as 10 rpm and at an initial nutation angle up to 30 deg. This suggests that the technique of "decoupling" the spin rate and the transverse rate may have general application to spinners with an almost symmetrical spin configuration ($I_x \cong I_y$).

The performance of the spin-down and active nutation controller at low spin rates was also found to be satisfactory. The spin-down can be terminated within an accuracy of 2% from the required final spin rate. The estimated transverse rate closely follows the actual rate, even if the accelerometer's resolution is no better than 0.002 m/s/bit. Note that for the given resolution, the output of the ACC at 1 rpm will not change more than 5 bits in 30 s at a 2-deg nutation angle.

The effect of energy dissipation was simulated by including additional terms in the rigid body dynamical equations to account for the energy dissipation effects. The model has the property of conserving the total angular momentum, while dissipating the energy at a given rate.

Acknowledgments

The research described in this paper was performed at Jet Propulsion Laboratory, California Institute of Technology, under contract with the National Aeronautics and Space Administration.

Refrences

[1] Grasshoff, L.H., "An Onboard, Closed-Loop, Nutation Control System for a Spin-Stabilized Spacecraft," *Journal of Spacecraft and Rockets,* Vol. 5, May 1968, pp. 530-535.

[2] Beard, M.B. and Plett, M., "Spacecraft Nutation," *Spacecraft Attitude Determination and Control,* D. Reidel Publishing Company, Dordrecht, Holland, 1978, pp. 534-548.

[3] Detchmendy, D.M. and Sridhar, R., "Sequential Estimation of States and Parameters in noisy Nonlinear Dynamical Systems," *Journal of Basic Engineering,* Vol. 88, June 1966, pp. 362-368.